Geomechanics and Engineering, *Vol. 37, No. 1 (2024) 85-95*
https://doi.org/10.12989/gae.2024.37.1.085

Static and dynamic characteristics of silty sand treated with nano-silica and basalt fiber subjected to freeze-thaw cycles

Hamid Alizadeh Kakroudi[a], Meysam Bayat* and Bahram Nadi[b]

Department of Civil Engineering, Najafabad Branch, Islamic Azad University, Najafabad, Iran

(*Received April 19, 2023, Revised March 19, 2024, Accepted March 30, 2024*)

Abstract. This study investigates the influence of nano-silica and basalt fiber content, curing duration, and freeze-thaw cycles on the static and dynamic properties of soil specimens. A comprehensive series of tests, including Unconfined Compressive Strength (UCS), static triaxial, and dynamic triaxial tests, were conducted. Additionally, scanning electron microscopy (SEM) analysis was employed to examine the microstructure of treated specimens. Results indicate that a combination of 1% fiber and 10% nano-silica yields optimal soil enhancement. The failure patterns of specimens varied significantly depending on the type of additive. Static triaxial tests revealed a notable reduction in the brittleness index (IB) with the inclusion of basalt fibers. Specimens containing 10% nano-silica and 1% fiber exhibited superior shear strength parameters and UCS. The highest cohesion and friction angle were obtained for treated specimens with 10% nano-silica and 1% fiber, 90 kPa and 37.8°, respectively. Furthermore, an increase in curing time led to a significant increase in UCS values for specimens containing nano-silica. Additionally, the addition of fiber resulted in a decrease in IB, while the addition of nano-silica led to an increase in IB. Increasing nano-silica content in stabilized specimens enhanced shear modulus while decreasing the damping ratio. Freeze-thaw cycles were found to decrease the cohesion of treated specimens based on the results of static triaxial tests. Specimens treated with 10% nano-silica and 1% fiber experienced a reduction in shear modulus and an increase in the damping ratio under freeze-thaw conditions. SEM analysis reveals dense microstructure in nano-silica stabilized specimens, enhanced adhesion of soil particles and fibers, and increased roughness on fiber surfaces.

Keywords: basalt fiber; dynamic properties; freeze-thaw; nano-silica; triaxial; UCS

1. Introduction

In civil engineering projects, the compressive strength, shear strength parameters (cohesion, c, friction angle, ϕ), and dynamic properties (shear modulus, G, damping ratio, D) of geomaterials are crucial for structural design. Over time, various additives, such as traditional stabilizers (like lime and cement) and natural or synthetic fibers, have been proposed to enhance the static and dynamic properties of weak and soft soils in civil engineering endeavors. A persistent challenge in these projects remains the high compressibility or low shear strength parameters and dynamic characteristics of geomaterials (Zhang *et al.* 2016, Du and Pang 2020, Phanikumar and Ramanjaneya Raju 2020, Bian *et al*. 2021, Sharma and Kumar 2021, Momeni Bayat and Ajalloeian 2022, Salehi *et al.* 2022, Rezaei-Hosseinabadi *et al.* 2022). The effectiveness of soil improvement methods on the static and dynamic characteristics of geomaterials hinges on their geotechnical properties. Cement or lime stabilization enhances the static and dynamic characteristics of granular soils by reducing void spaces and introducing bonding agents between granular particles (Aryal and Kolay 2020, Ghadir and Ranjbar 2018, Liu *et al.* 2019, Sukmak *et al*. 2019). However, soils stabilized with cement or lime often exhibit extremely brittle behavior due to their low tensile strength (Bayat *et al*. 2013, Ghanbari and Bayat 2022, Hadi Sahlabadi *et al.* 2021, ShahriarKian *et al.* 2021).

Previous studies have highlighted a significant enhancement in geotechnical parameters, such as the ductility of stabilized soils, through the incorporation of fibers (Anggraini *et al.* 2015, Boz *et al.* 2018, Estabragh *et al.* 2017, Olgun 2013, Pongsivasathit *et al.* 2019). (Tang *et al.* 2007) observed that fiber inclusion increased the unconfined compressive strength (UCS), both shear strength parameters, and failure strain levels of cement-stabilized specimens. Narani *et al*. (2021) demonstrated that the mechanical behavior of cement-stabilized rammed-earth composites can be enhanced by incorporating fibers under cyclic loading conditions. Cao *et al.* (2019) investigated the effect of fiber inclusion on the static and dynamic characteristics of stabilized soil with cement and fly ash, revealing significant improvements in compressive strength, dynamic characteristics, and energy absorption capacity with an optimal fiber content of 0.6%.

In contemporary civil engineering projects, the integration of nanomaterials with unique chemical and physical properties has become increasingly significant. Particularly in geotechnical projects, the adoption of nanomaterials aims to enhance soil response (Eshaghzadeh *et al*. 2021, Jassem and Tabarsa 2015, Shokrieh *et al*. 2013,

*Corresponding author, Associate Professor
E-mail: bayat.m@pci.iaun.ac.ir
[a]Ph.D Student
[b]Ph.D.

http://www.techno-press.org/?journal=gae&subpage=7
ISSN: 2005-307X (Print), 2092-6219 (Online)

Tomar *et al.* 2019, Turku and Kärki 2014). Lv *et al.* (2018) observed a notable improvement in the geotechnical characteristics of loess soil through the incorporation of SiO_2. Gao *et al.* (2020) conducted resonant-column tests, revealing a proportional increase in shear modulus with the addition of nano-MgO in silty clay. Heidarizadeh *et al.* (2021) performed bender element tests, showing a significant rise in maximum shear modulus with increased cement or SiO_2 content and curing time in soft clay stabilization. Thomas and Rangaswamy (2020) investigated the dynamic properties of nanoparticles and bioenzyme stabilized soft clay using cyclic triaxial apparatus, suggesting a novel mixture of nano-silica, bioenzyme, and cement for enhancing soil dynamics. Prior research suggests that nontraditional additives can serve as partial or complete replacements for cement or lime in soil stabilization, addressing environmental concerns (Al-Mansob *et al.* 2021, Arora 2019, Jiang *et al*. 2022, Kulanthaivel *et al*. 2021).

The static and dynamic properties of treated geomaterials are influenced by various factors, including additive type and content, confining pressure, freeze-thaw or wet-dry cycles, frequency, stress anisotropy, and shear strain level (Bayat 2021, Chittoori et al. 2018, Choobbasti *et al.* 2019, Jahandari *et al.* 2017, Pu 2021). When subjected to freeze-thaw cycles, the static and dynamic characteristics of reinforced or stabilized soils undergo significant changes due to moisture migration and ice formation within soil voids (Bozbey *et al.* 2018, Chaduvula *et al*. 2014, Elif Orakoglu *et al*. 2017, Hadi Sahlabadi *et al*. 2021, Kalhor *et al.* 2019, Qi *et al*. 2008, Shibi and Kamei 2014, Wang *et al.* 2015). Hence, investigating the engineering properties of geomaterials under freeze-thaw conditions is essential. Cheng *et al*. (2021) s examined the impact of freeze-thaw cycles through a series of consolidated undrained triaxial shear tests, revealing a gradual reduction in shear strength with an increasing number of freeze-thaw cycles. Yousefi *et al.* (2022) investigated the dynamic characteristics of nano-cement stabilized soils, finding a decrease in shear modulus with an increasing number of freeze-thaw cycles. However, the inclusion of nano-cement resulted in an increased shear modulus and decreased damping ratio. Chen *et al.* (2022) suggested nano-MgO as a suitable additive for stabilizing geomaterials under freeze-thaw conditions. (Jiang *et al.* 2022) investigated the flexural behavior and energy dissipation of cement-based iron tailings powder (CITP) modified with polypropylene (PP) and glass fibers under freeze-thaw cycles. Findings demonstrate a decline in flexural strength for both PP-CITP and GCITP with increased freeze-thaw cycles, highlighting GCITP's superior frost resistance.

The integration of nano materials and fibers represents a promising avenue for soil improvement. Fibers and nano-silica enhance tensile strength, durability, and overall soil properties. Fibers reinforce soil, while nano materials fill voids, strengthen interparticle bonds, and enhance shear strength. This combined approach offers a cost-effective, sustainable solution for soil stabilization, yielding improved performance and durability.

While numerous studies have explored the impact of fiber and nanoparticle incorporation, as well as freeze-thaw cycles, on the static and dynamic properties of geomaterials, there remains a gap in understanding the static and dynamic behavior of soils enhanced with a combination of basalt fiber and nano-silica. In this study, we address this gap by investigating the effects of basalt fiber content, nano-silica content, and freeze-thaw cycles on the UCS, shear strength parameters, and dynamic properties of silty sand treated with nano-silica and basalt fiber.

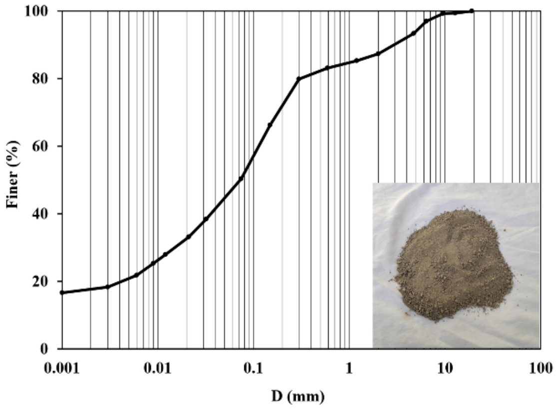

Fig. 1 Grain size distribution curve of Varzaneh sand

2. Materials, test apparatus, and testing procedure

In this study, Varzaneh sand sourced from Isfahan, characterized by fine and sub-rounded particles, was utilized. Soil classification is a fundamental process in geotechnical engineering that involves categorizing soils based on their physical and mechanical properties. This classification is typically conducted through a series of laboratory tests and field observations aimed at characterizing soil behavior and determining its engineering properties. Common methods used for soil classification include grain size analysis to assess particle distribution, Atterberg limits tests to evaluate soil plasticity and liquidity limits, and various other tests to determine parameters such as soil density, permeability, and compressibility. By systematically classifying soils into distinct categories according to standardized classification systems such as the Unified Soil Classification System (USCS) or the American Society for Testing and Materials (ASTM) standards, engineers and researchers can better understand soil behavior, make informed decisions regarding construction projects, and predict potential geotechnical challenges. Varzaneh sand is classified as silty sand (SM) according to the USCS. Fig. 1 displays the particle size distribution curve and a photo of Varzaneh sand. The geotechnical and physical properties of Varzaneh sand are detailed in Table 1. Basalt fiber, ranging from 0% to 4% by weight, served as the reinforcement material. Table 2 presents the physical and mechanical properties of the basalt fibers. Nano-silica, with proportions ranging from 0% to 20% by weight, was employed as the stabilizer material, with its physical and chemical properties outlined in Table 3.

Table 1 Geotechnical and physical properties of Varzaneh sand

Characteristics	Values and descriptions
Specific gravity	2.66
Passing No. 200 sieve (%)	20
Plasticity index (%)	NP
Unified Soil Classification System (USCS)	SM
Optimum water content (%)	9.55
Maximum dry unit weight (kN/m^3)	20.11
Cohesion (kPa)	15
Friction angle (°)	35

Table 2 Physical and mechanical properties of the tire textile fibres

Property	Value
Cut length (mm)	10
Filament diameter (μm)	17
Density (g/cm3)	2.61
Elastic modulus (GPa)	95
Tensile strength (MPa)	3000

Table 3 Physical and chemical properties of nano-silica particles

Property/composition	Value
Specific surface area (m^2/g)	235
Main particle size (μm)	25
Agglomerate mean particle size (μm)	10.5
Tamped density (kg/m^3)	200
pH	6.8
SiO_2 (%)	>98.5
SO_3 (%)	0.5

A series of tests including UCS, static triaxial, and cyclic triaxial tests were conducted to evaluate the compressive strength, shear strength parameters, and dynamic properties of the specimens. UCS specimens measuring 50 mm in diameter and 100 mm in height were prepared and tested according to ASTM D-2166 at a constant strain rate of 1% per minute until peak stress was reached. Cylindrical specimens measuring 100 mm in diameter and 200 mm in height (with a height-to-diameter ratio of 2) were prepared for static and cyclic triaxial tests, following ASTM D-4767 and ASTM D-3999 standards, respectively.

The triaxial compressive strength test serves as an indirect method for assessing shear strength parameters. By subjecting soil specimens to controlled axial and radial stresses in a triaxial cell, this test allows for the determination of parameters such as cohesion and internal friction angle, which are indicative of the material's shear strength characteristics. Through the analysis of stress-strain relationships and failure modes observed during the test, valuable insights into the mechanical behavior of the soil under various loading conditions can be gained, aiding in the characterization of its shear strength properties.

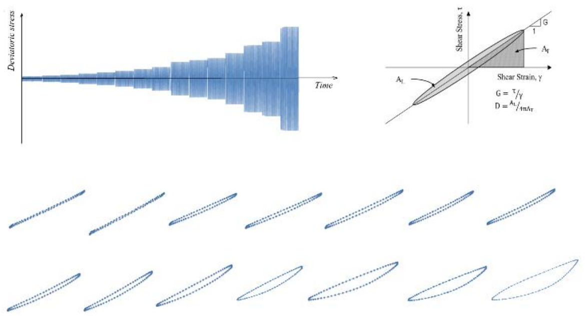

Fig. 2 Procedure defined by ASTM D-3999 using hysteresis loops to extract the dynamic properties of specimens

During static triaxial tests, specimens were sheared at a constant strain rate of 1 mm/min until the axial strain reached approximately 20%. Dynamic properties were determined following the procedure outlined in ASTM D-3999, using hysteresis loops to extract dynamic properties for shear strain amplitudes ranging from 10^$^{-4}$ to 10^$^{-2}$ (see Fig. 2). Cyclic triaxial tests involved stages of cyclic loading starting at a small shear strain level with a sinusoidal wave at a constant frequency of 1 Hz, gradually increasing in magnitude. Each stage comprised 40 loading cycles, with the tenth cycle of hysteresis loops utilized to compute shear modulus and damping ratio. Local Linear Variable Differential Transformers (LVDTs) were installed on the membrane during triaxial tests to measure axial strain.

In general, the dynamic properties of geomaterials have been studied for various confining pressures ranging from 50 kPa to 500 kPa (Bayat 2020a, b, Thomas and Rangaswamy 2020, Yousefi *et al*. 2022). However, in this study, we opted for a confinement pressure of 200 kPa for measuring the shear modulus and damping ratio of treated specimens with varying nano and fiber content to assess their effects. Soil improvement is typically implemented at the surface of the ground, where the overall stress around the soil element is relatively limited and low due to the shallow depth of the soil above it. Therefore, by selecting a confinement pressure of 200 kPa, we aimed to simulate conditions relevant to practical soil improvement applications while focusing on the dynamic response of the treated soil under controlled laboratory conditions.

To determine the maximum dry density (MDD) and optimum moisture content (OMC) of various material mixtures, standard Proctor compaction tests were conducted initially. Varzaneh sand was oven-dried at 110°C for 24 hours, followed by the addition of the desired number of additives (nano-silica and basalt fiber) and thorough mixing using a mixer machine (see Fig. 3). Subsequently, water equivalent to the OMC was sprayed onto the materials and mixed again to ensure uniform water distribution. All specimens were prepared at MDD with initial water content equal to OMC using a wet tamping technique into the mold in five layers for UCS and static and cyclic triaxial tests.

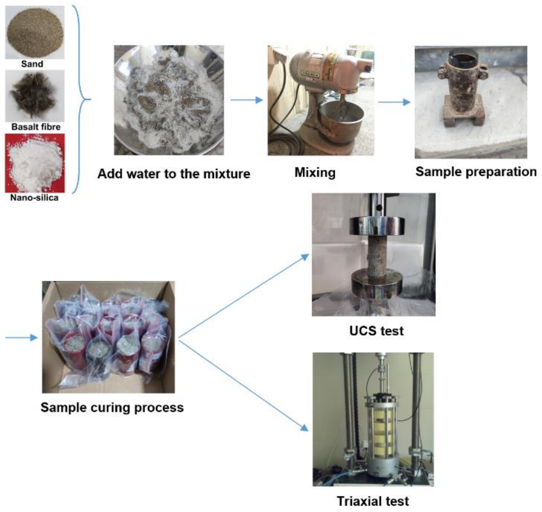

Fig. 3 Process of preparing specimens for testing

The wet tamping method offers significant advantages for preparing treated soil specimens with nanomaterials and fibers in this study. Firstly, by saturating the soil with water before compaction, the wet tamping process ensures thorough dispersion and distribution of the nanomaterials and fibers within the soil matrix, promoting uniformity in treatment application. This uniform distribution is crucial for accurately assessing the effectiveness of the treatment on soil properties such as strength and durability. Additionally, wet tamping facilitates better bonding between the soil particles and the introduced nanomaterials and fibers, enhancing the overall stability and mechanical properties of the treated soil. Furthermore, the controlled compaction achieved through wet tamping helps mitigate potential issues such as segregation or uneven distribution of the treatment components, ensuring consistent results across the reconstituted soil specimens. Overall, the wet tamping method provides a reliable and reproducible approach for preparing treated soil specimens, enabling precise evaluation of the effects of nanomaterials and fibers on soil behavior and performance.

Specimens containing nano-silica were wrapped with thin plastic film and stored in a humidity chamber for 7, 14, 28, 60, or 90 days, while specimens without nano-silica were tested promptly.

To investigate the impact of freeze-thaw cycles on shear strength parameters, a closed system was employed. Specimens were initially stored in a freezer at -20°C for a minimum of 12 hours for freezing, followed by thawing at 20°C for at least 12 hours. This temperature range for freeze-thaw cycles aligns with previous studies (Hadi Sahlabadi *et al*. 2021, Roustaei *et al*. 2021, Torabi Asl and Taherabadi 2018). Specimens were tested after 0, 1, 3, 6, or 9 cycles of freezing-thawing.

3. Tests results and discussion

3.1 UCS tests

Before examining the combined impact of basalt fibers and nano-silica, the optimal content for each was determined individually through initial testing. This selection aimed to achieve the desired improvements in soil properties. Subsequent tests evaluated the synergistic effects of the combined additives on soil enhancement. This approach allowed for a comprehensive assessment of their individual and combined contributions to soil improvement. The variation of UCS for fiber-reinforced specimens with different fiber contents is illustrated in Fig. 4. The results demonstrate an increase in UCS with increasing fiber content from 0% to 1%. However, beyond 1% fiber content, the UCS shows a declining trend. This suggests that the optimal basalt fiber content is 1%, as further increases lead to a reduction in UCS. Fig. 5 displays the variation of UCS for nano-silica-stabilized specimens at various curing times up to 90 days. It is evident that, for a given curing time, specimens stabilized with 10% nano-silica exhibit the highest UCS values. Moreover, UCS gradually increases with increasing curing time from 7 to 90 days. Fig. 6(a) depicts the effect of nano-silica and fiber content on the UCS of specimens treated with both materials at a curing time of 28 days. The results indicate that specimens containing 10% nano-silica and 1% fiber demonstrate higher UCS compared to other specimens for a given curing age. Furthermore, Fig. 6(b) illustrates the effect of curing time on UCS values for specimens treated with 10% nano-silica and 1% fiber. It is observed that UCS significantly increases with increasing curing time from 7 to 28 days. Overall, the results of the UCS tests highlight 1% fiber and 10% nano-silica as the optimum mixture percentages for enhancing UCS properties.

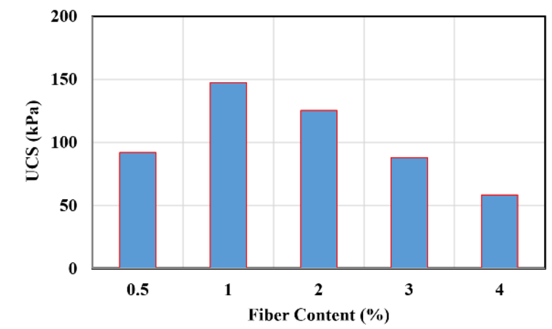

Fig. 4 UCS results of the fiber reinforced specimens at various fiber content

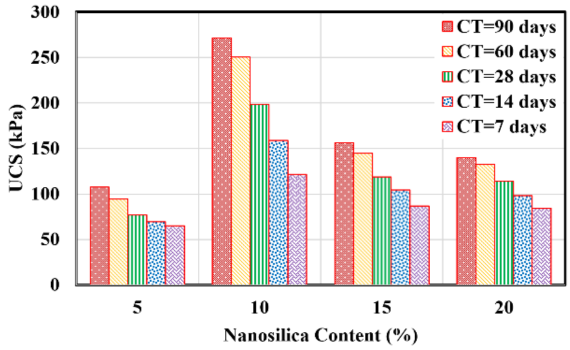

Fig. 5 UCS results of the nano-silica stabilized specimens at various nano-silica content and curing time

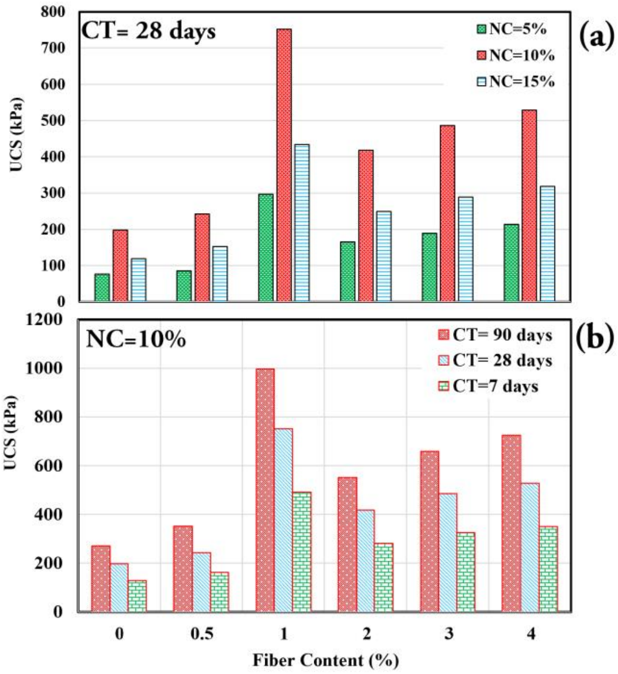

Fig. 6 UCS results of the specimens treated with nano-silica and fiber at (a) curing time of 28 days (b) various curing time and nano-silica content of 10%

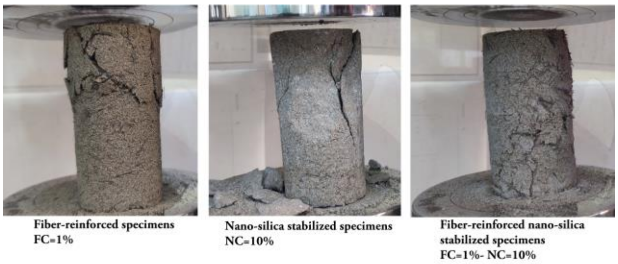

Fig. 7 Failure patterns of the specimens at the end of the UCS test

The failure patterns of specimens, along with the shapes, sizes, arrangements, and distributions of cracks, serve as crucial evidence primarily influenced by the movement and sliding of soil particles, deflection, and internal particle stress (Ghanbari and Bayat 2022). Fig. 7 illustrates the failure patterns of three types of specimens: fiber-reinforced, nano-silica stabilized, and fiber-reinforced nano-silica stabilized specimens.

In the fiber-reinforced specimens, small-sized cracks are observed primarily in the upper section. Conversely, in the nano-silica stabilized specimens, a prominent longitudinal crack traverses the entirety of the specimen, accompanied by smaller cracks at the top, alongside debris and soil blocks. Notably, cracks in the nano-silica stabilized specimens exhibit rapid development. The incorporation of fibers significantly influences the failure pattern of the nano-silica stabilized specimens, enhancing their brittle behavior by reducing crack length and increasing the occurrence of fine cracks.

Indeed, the fibers exhibit a notable "bridging" effect, dispersing stress, forming a stable three-dimensional network, and impeding crack propagation within the specimens. Previous studies have consistently demonstrated the efficacy of various fiber types in enhancing the brittle behavior of stabilized specimens (Estabragh *et al*. 2017, Ghanbari and Bayat 2022, Kaniraj and Havanagi 2001, Tang *et al*. 2007, Yilmaz and Ozaydin 2013).

3.2 Static triaxial tests

A series of static triaxial tests were conducted to investigate the mechanical characteristics of the specimens. Initially, tests were performed under a confining pressure of 200 kPa to examine the influence of basalt fiber and nano-silica contents on the maximum deviatoric stress and brittleness index (IB). The brittleness index, defined as the ratio of peak deviatoric stress to ultimate (or residual-state) deviatoric stress, was analyzed (Bahadori *et al.* 2008, Güllü and Khudir 2014, Liu *et al*. 2020, Wang *et al.* 2021).

Fig. 8(a) presents the variation of maximum deviatoric stress and brittleness index for fiber-reinforced specimens. The specimen containing 1% fiber exhibited the highest maximum deviatoric stress, while the addition of fibers reduced the brittleness index, approaching zero. Similar findings have been reported in previous studies (Consoli *et al*. 2007, Radoslaw *et al*. 2005).

Fig. 8(b) illustrates the variation of maximum deviatoric stress and brittleness index for nano-silica stabilized specimens. Specimens stabilized with 10% nano-silica demonstrated the highest maximum deviatoric stress, with the nano-silica content significantly impacting this stress. The brittleness index decreased with increasing nano-silica content up to 10% and then stabilized. Comparison with fiber-reinforced specimens showed that nano-silica stabilized specimens exhibited higher maximum deviatoric stress values.

Fig. 8(c) shows the variation of maximum deviatoric stress and brittleness index for specimens treated with 10% nano-silica and different fiber percentages. These specimens exhibited the highest maximum deviatoric stress, with the 1% fiber content specimen displaying the highest value. Overall, fiber addition reduced the brittleness index and improved mechanical behavior.

Subsequent static triaxial tests were conducted under confining pressures of 100, 200, and 400 kPa to analyze shear strength parameters. The selection of 100, 200, and 400 kPa for static triaxial tests aligns with common geotechnical practices. These pressures simulate real-world conditions in embankments, foundations, and retaining structures. Testing under these pressures offers insights into the mechanical behavior of treated soils. Mohr-Coulomb failure envelopes of various specimens, including sand, fiber-reinforced, nano-silica stabilized, and fiber-reinforced nano-silica stabilized specimens, were plotted (see Fig. 9). The results indicate that the addition of nano-silica and fiber had minimal effect on the friction angle, while significant changes were observed in cohesion. Specimens containing 10% nano-silica and 1% fiber exhibited the highest cohesion and friction angle, highlighting the significant impact of nano-silica on cohesion. Specifically, cohesion increased from 15 to 90 with the addition of 10% nano-silica and 1% fiber to sand specimens.

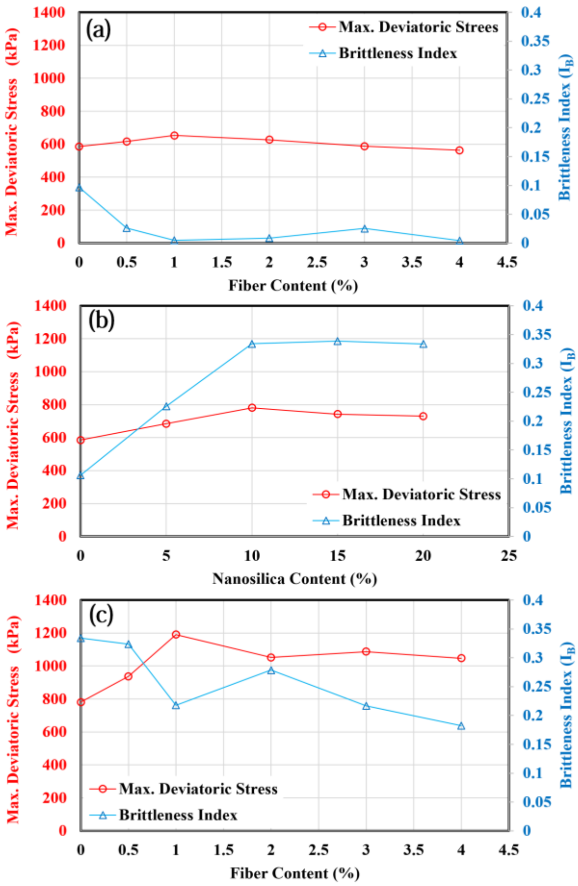

Fig. 8 Variations of maximum deviatoric stress and brittleness index (IB) versus different additive contents (a) the fiber reinforced specimens, (b) the nano-silica stabilized specimens and (c) the specimens treated with 10% nano-silica and various fiber contents

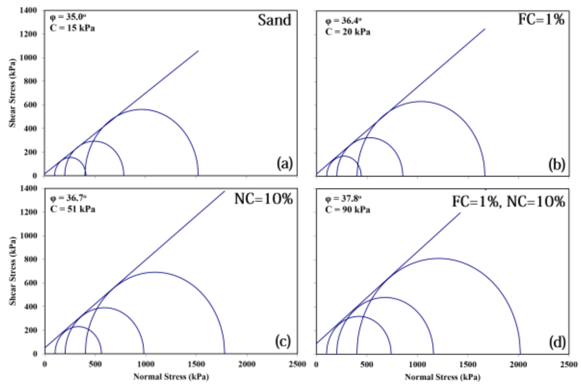

Fig. 9 Mohr-Coulomb failure envelopes of specimens (a) the pure sand, (b) the fiber reinforced specimen with 1% fiber, (c) the nano-silica stabilized specimen with 10% nano-silica and (d) the specimens treated with 10% nano-silica and 1% fiber

3.3 Cycles triaxial tests

This section presents the results of cyclic triaxial tests, focusing on the changes in shear modulus and damping ratio versus shear strain under a confining pressure of 200 kPa.

Fig. 10 displays the shear modulus reduction and damping ratio curves of nano-silica stabilized specimens. The stabilized specimens demonstrate slightly more nonlinear behavior compared to pure sand specimens. Shear modulus reduction curves for stabilized specimens are significantly higher than those for pure sand specimens, with specimens containing 10% nano-silica exhibiting the highest shear modulus. The maximum shear modulus of specimens treated with 10% nano-silica is approximately 2.5 times higher than that of pure sand specimens. Shear modulus increases with nano-silica content up to 10% and then decreases with further increases in nano-silica content. Additionally, stabilized specimens exhibit lower damping ratios compared to pure sand specimens, with the maximum damping ratio being approximately 6% higher for pure sand specimens. Increasing nano-silica content from 5 to 20% has little effect on the damping ratio, resulting in close damping ratio curves for nano-silica stabilized specimens.

Fig. 11 illustrates the shear modulus reduction and damping ratio curves of fiber-reinforced specimens. Fiber content significantly influences the results, with reinforced specimens showing slightly more linear behavior compared to pure sand specimens. Specimens containing 1% fiber exhibit the highest shear modulus and damping ratio among reinforced specimens. Comparison with nano-silica stabilized specimens indicates that nano-silica stabilized specimens have higher shear modulus, while fiber-reinforced specimens exhibit higher damping ratio. Additionally, fiber content has a greater effect on damping ratio compared to nano-silica content, consistent with previous findings (Li and Senetakis 2017).

Fig. 12 presents the shear modulus reduction and damping ratio curves of specimens treated with a mixture of nano-silica and fiber. The specimen containing 10% nano-silica and 1% fiber demonstrates the highest shear modulus.

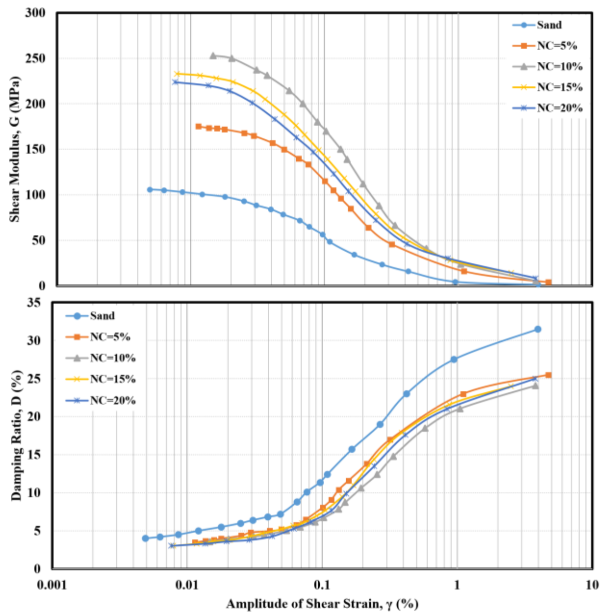

Fig. 10 Variation of shear modulus and damping ratio of nano-silica stabilized specimens as a function of shear modulus (σ_3= 200 kPa)

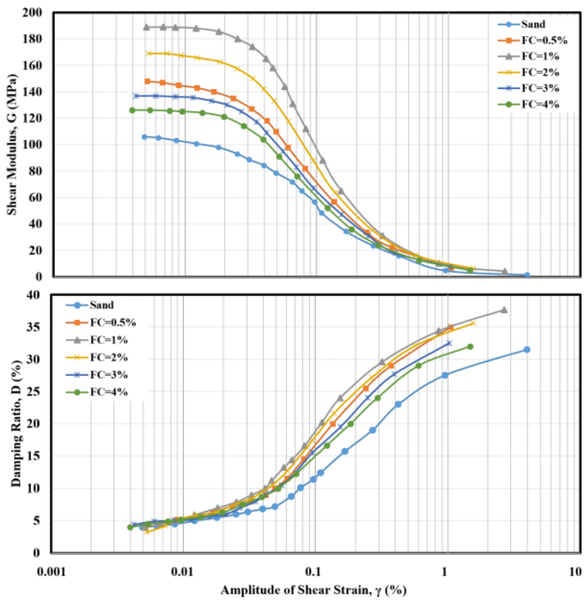

Fig. 11 Variation of shear modulus and damping ratio of fiber reinforced specimens as a function of shear modulus (σ_3= 200 kPa).

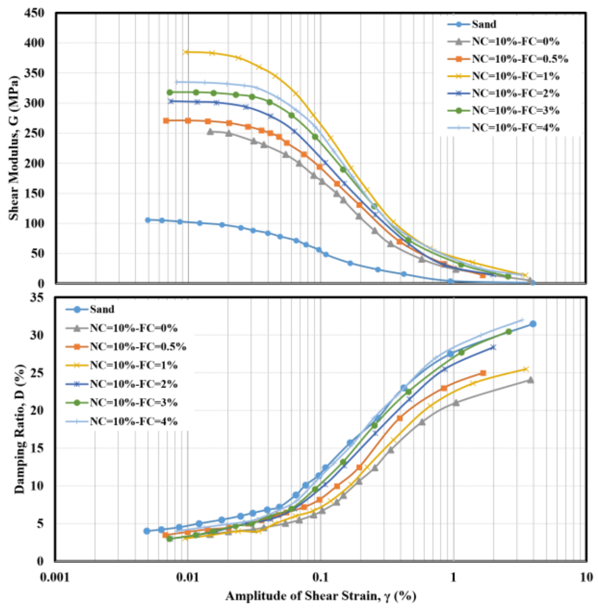

Fig. 12 Variation of shear modulus and damping ratio of specimens treated with nano-silica and fiber as a function of shear modulus (σ_3= 200 kPa)

Overall, specimens treated with a combination of nano-silica and fiber exhibit larger shear modulus values compared to both nano-silica stabilized and fiber-reinforced specimens.

3.4 Freeze-thaw cycles

A series of static triaxial tests were conducted to investigate the effect of freeze-thaw cycles on the shear strength parameters of specimens.

Fig. 13 illustrates the impact of freeze-thaw cycles on the reduction of shear strength parameters. The friction

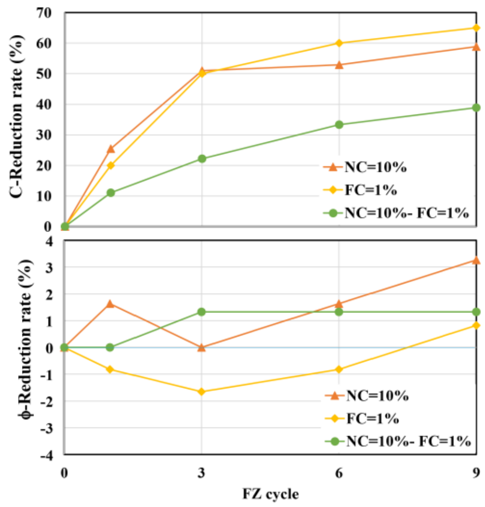

Fig. 13 Effect of freeze-thaw cycles on the reduction of shear strength parameters.

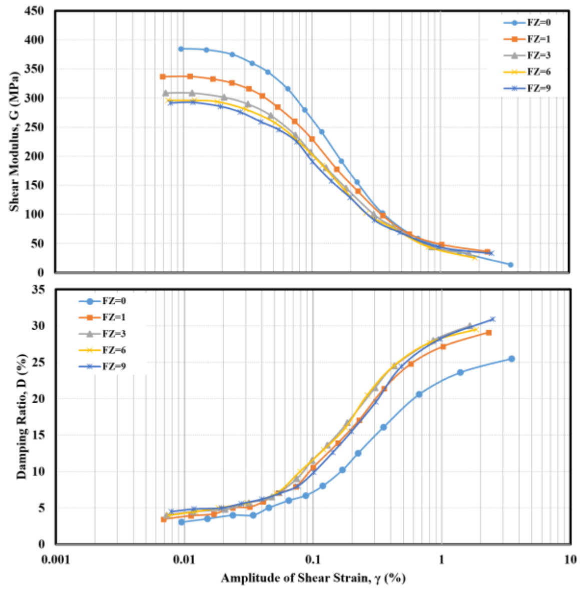

Fig. 14 Effect of freeze-thaw cycles on the shear modulus and damping ratio of the specimens treated with 10% nano-silica and 1% fiber (σ_3= 200 kPa)

angle shows minimal variation due to freeze-thaw cycles, with changes less than 4%. However, specimens containing nano-silica experienced an increase in the friction angle, while a decrease was observed in specimens containing only fibers. Freeze-thaw cycles significantly reduce cohesion in all specimens, with specimens treated with 10% nano-silica and 1% fiber exhibiting the lowest reduction, and reinforced specimens with 1% fiber showing the highest reduction.

Fig. 14 presents the effect of freeze-thaw cycles on the shear modulus reduction and damping ratio curves of specimens treated with 10% nano-silica and 1% fiber under a confining pressure of 200 kPa. The results highlight the significant impact of freeze-thaw cycles on the dynamic properties of specimens. Shear modulus at shear strain around 0.01% decreases from 390 MPa to 290 MPa with increasing freeze-thaw cycles from 0 to 9. Shear modulus

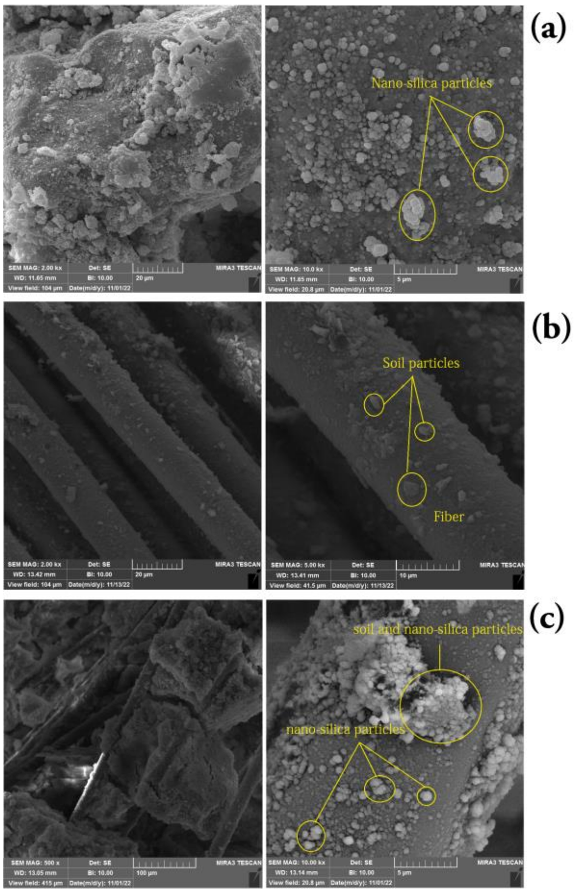

Fig. 15 SEM images of (a) the nano-silica stabilized specimens, (b) the fiber reinforced specimens and (c) the specimen treated with nano-silica and fiber

loss primarily occurs in the initial freeze-thaw cycles. Conversely, the damping ratio corresponding to large shear strain values increases from 25.5% to 31% with increasing freeze-thaw cycles from 0 to 9. Initial freeze-thaw cycles notably affect the damping ratio of specimens. These findings align with previous studies by (Chen *et al.* 2022, Elif Orakoglu *et al*. 2017, Yousefi *et al*. 2022).

3.5 SEM analyses

Previous studies have highlighted that the static or dynamic behavior of reinforced or stabilized soils with various additive materials is significantly influenced by the microscopic characteristics of mixtures (Hadi Sahlabadi *et al.* 2021, Tang *et al.* 2007).

Fig. 15(a) presents SEM micrographs of nano-silica stabilized specimens with a nano-silica content of 10%. The images reveal a dense microstructure resulting from the presence of nano-silica particles, forming a paste that exhibits strong adhesion to sand particles. Additionally, increased roughness on the surface of sand particles and reduced voids between particles are observed. In Fig. 15(b), SEM micrographs of fiber-reinforced specimens with a fiber content of 1% are displayed. The images illustrate the penetration of soil particles onto the fiber surface, enhancing contact between fibers and soil particles. Fibers play a crucial role in providing tension within the mixture through fiber bridging, particularly when cracks propagate. Fig. 15(c) depicts SEM micrographs of treated specimens with a nano-silica content of 10% and a fiber content of 1%. Enhanced adhesion of soil particles and nano-silica paste to the fiber surface is evident, along with increased attachment by cementitious particles. This results in greater roughness on the fiber surface, facilitating more contact points, interlocking, and bond strength between fibers and soil particles. Ultimately, the increased roughness of fibers enhances interactions between fibers and sand particles, contributing to improved performance. These observations underscore the importance of microscopic scale characteristics in understanding the behavior of reinforced or stabilized soils with additive materials.

4. Conclusions

In this study, a comprehensive series of tests, including UCS, static and dynamic triaxial tests, were conducted to assess the impact of basalt fiber content, nano-silica content, and freeze-thaw cycles on the mechanical and dynamic behavior of Varzaneh sand. Additionally, SEM micrographs were utilized to corroborate the test results. The key findings and conclusions drawn from this research are summarized as follows:

1. The UCS of fiber-reinforced specimens increased with fiber content up to 1%, beyond which it declined. The maximum UCS, approximately 150 kPa, was observed at 1% fiber content. Nano-silica stabilized specimens with 10% nano-silica exhibited the highest UCS (approximately 260 kPa) at a curing time of 90 days, with a gradual increase observed with longer curing times. A combination of 1% fiber and 10% nano-silica proved to be the optimum mixture for soil improvement, showing significantly higher UCS compared to specimens treated with either fiber or nano-silica alone.
2. Fiber reinforcement improved the brittle behavior of nano-silica stabilized specimens, reducing crack length and increasing the number of fine cracks.
3. Specimens with 1% fiber exhibited the highest maximum deviatoric stress among fiber-reinforced specimens, while those stabilized with 10% nano-silica showed the highest values among nano-silica stabilized specimens. A significant reduction in the brittleness index was observed with fiber reinforcement. Specimens treated with a mixture of fiber and nano-silica exhibited higher maximum deviatoric stress values compared to those treated with either fibers or nano-silica alone.
4. Friction angle changes due to fiber or nano-silica addition were minimal, while significant changes in cohesion were observed. The highest friction angle and cohesion were observed in specimens containing 10% nano-silica and 1% fiber.
5. Nano-silica stabilized specimens exhibited slightly more nonlinear behavior compared to pure sand specimens, with significantly higher shear modulus. Fiber-reinforced specimens showed more linear behavior, with specimens containing 1% fiber exhibiting the highest shear modulus and damping ratio.

6. Freeze-thaw cycles had a significant effect on cohesion reduction, with the lowest reduction observed in specimens treated with 10% nano-silica and 1% fiber. Dynamic properties were affected by freeze-thaw cycles, with a decrease in shear modulus and an increase in damping ratio observed as cycles increased.

7. SEM micrographs revealed dense microstructures and strong adhesion between sand particles and nano-silica gel, resulting in decreased voids. Fiber-reinforced specimens showed enhanced adhesion between soil particles and fibers, leading to improved interactions.

References

Al-Mansob, R.A., Wong, W.F., Alsharef, J.M.A., Jassam, T.M., Ng, J.L., Albrka Ali, S.I. and Yusof, Z.B. Md. (2021), "Unconfined compressive strength characteristic of soft soil mixed with lime and nano alumina", *AIP Conference Proceedings* 2401. https://doi.org/10.1063/5.0073026.

Anggraini, V., Asadi, A., Huat, B.B.K. and Nahazanan, H. (2015), "Effects of coir fibers on tensile and compressive strength of lime treated soft soil", *Measurement*, **59**, 372-381. https://doi.org/10.1016/j.measurement.2014.09.059.

Arora, A., Singh, B. and Kaur, P. (2019), "Performance of nano-particles in stabilization of soil: A comprehensive review", *Materials Today: Proceedings*, **17**, 124-130. https://doi.org/10.1016/j.matpr.2019.06.409.

Aryal, S. and Kolay, P.K. (2020), "Long-term durability of ordinary portland cement and polypropylene fibre stabilized Kaolin soil using wetting–drying and freezing–thawing test", *Int. J. Geosynthetics Ground Eng.*, **6**(1), 1-15. https://doi.org/10.1007/s40891-020-0191-9.

Asl, M.T. and Taherabadi, E. (2018), "Modification of silty clay strength in cold region's pavement using glass residue", *Cold Reg. Sci. Tech*., **154**, 11-19. https://doi.org/10.1016/j.coldregions.2018.06.005.

Bahadori, H., Ghalandarzadeh, A. and Towhata, I. (2008), "Effect of non plastic silt on the anisotropic behavior of sand", *Soils Found*., **48**(4), 531-545. https://doi.org/10.3208/sandf.48.531.

Bayat, M., Asgari, M.R. and Mousivand, M. (2013), "Effects of cement and lime treatment on geotechnical properties of a low plasticity clay", *Proceedins of the International Conference on Civil Engineering Architecture & Urban Sustainable Development*, 27-28 November, Tabriz, Iran Effects.

Bayat, M. (2020a), "Effect of sand fouling on the dynamic properties and volume change of gravel during cyclic loadings", *Periodica Polytechnica Civil Eng.*, https://doi.org/10.3311/PPci.15857.

Bayat, M. (2020b), "Universal model forms for predicting the dynamic properties of granular soils", *Acta Geodynamica et Geomaterialia*, 217-227. https://doi.org/10.13168/AGG.2020.0016.

Bayat, M. (2021), "Shear wave velocity in granular soil considering effects of inherent and stress-induced anisotropy", *J. Central South Univ.*, **28**(5), 1476-1492. https://doi.org/10.1007/s11771-021-4711-0.

Bian, X., Zeng, L., Li, X., Shi, X., Zhou, S. and Li, F. (2021), "Fabric changes induced by super-absorbent polymer on cement–lime stabilized excavated clayey soil", *J. Rock Mech. Geotech. Eng.*, **13**(5), 1124-1135. https://doi.org/10.1016/j.jrmge.2021.03.006.

Boz, A., Sezer, A., Özdemir, T., Hızal, G.E. and Azdeniz Dolmacı, Ö. (2018), "Mechanical properties of lime-treated clay reinforced with different types of randomly distributed fibers", *Arabian J. Geosci*., **11**(6). https://doi.org/10.1007/s12517-018-3458-x.

Bozbey, I., Kelesoglu, M.K., Demir, B., Komut, M., Comez, S., Ozturk, T., Mert, A., Ocal, K. and Oztoprak, S. (2018), "Effects of soil pulverization level on resilient modulus and freeze and thaw resistance of a lime stabilized clay", *Cold Reg. Sci. Tech*., **151**, 323-334. https://doi.org/10.1016/j.coldregions.2018.03.023.

Cao, Z., Ma, Q. and Wang, H. (2019), "Effect of basalt fiber addition on static-dynamic mechanical behaviors and microstructure of stabilized soil compositing cement and fly ash", *Adv. Civil Eng.*, **2019**. https://doi.org/10.1155/2019/8214534.

Chaduvula, U., Desai, A.K. and Solanki, C.H. (2014), "Application of triangular polypropylene fibres on soil subjected to freeze-thaw cycles", *Indian Geotech. J.*, **44**(3), 351-256. https://doi.org/10.1007/s40098-013-0088-9.

Chen, S., Hou, X., Luo, T., Yu, Y. and Jin, L. (2022), Effects of MgO nanoparticles on dynamic shear modulus of loess subjected to freeze-thaw cycles", *J. Mater. Res. Tech*., **18**, 5019-5031. https://doi.org/10.1016/j.jmrt.2022.05.013.

Cheng, S., Wang, Q., Wang, J. and Han, Y. (2021), "Experimental study on undrained shear properties of saline soil under freeze-thaw cycles", *Geofluids*, **2021**. https://doi.org/10.1155/2021/9987414.

Chittoori, B.C.S., Puppala, A.J. and Pedarla, A. (2018), "Addressing clay mineralogy effects on performance of chemically stabilized expansive soils subjected to seasonal wetting and drying", *J. Geotech. Geoenviron. Eng*., **144**(1), 04017097. https://doi.org/10.1061/(asce)gt.1943-5606.0001796.

Choobbasti, A.J., Samakoosh, M.A. and Kutanaei, S.S. (2019), "Mechanical properties soil stabilized with nano calcium carbonate and reinforced with carpet waste fibers", *Constr. Build. Mater.,* **211**, 1094-1104. https://doi.org/10.1016/j.conbuildmat.2019.03.306.

Consoli, N.C., Heineck, K.S., Casagrande, M.D.T. and Coop, M.R. (2007), "Shear strength behavior of fiber-reinforced sand considering triaxial tests under distinct stress paths", *J. Geotech. Geoenviron. Eng*., **133**(11), 1466-1469. https://doi.org/10.1061/(asce)1090-0241(2007)133:11(1466).

Du, H. and Pang, S.D. (2020), "High-performance concrete incorporating calcined kaolin clay and limestone as cement substitute", *Constr. Build. Mater*., **264**. https://doi.org/10.1016/j.conbuildmat.2020.120152.

Eshaghzadeh, M., Bayat, M., Ajalloeian, R. and Hejazi, S.M. (2021), "Mechanical behavior of silty sand reinforced with nanosilica-coated ceramic fibers", *J. Adhesion Sci. Tech*., **35**(23), 2664-2683. https://doi.org/10.1080/01694243.2021.1898857.

Estabragh, A.R., Ranjbari, S. and Javadi, A.A. (2017), "Properties of clay soil and soil cement reinforced with polypropylene fibers", *ACI Mater. J*., **114**(2).

Gao, L., Luo, Y., Ren, Z., Yu, X. and Wu, K. (2020), "Experimental study on dynamic properties of Nano-MgO-modified silty clay", *Int. J. Geosynth. Ground Eng.*, **6**(2). https://doi.org/10.1007/s40891-020-00210-5.

Ghadir, P. and Ranjbar, N. (2018), "Clayey soil stabilization using geopolymer and Portland cement", *Constr. Build. Mater.*, **188**, 361-371. https://doi.org/10.1016/j.conbuildmat.2018.07.207.

Ghanbari, M. and Bayat, M. (2022), "Effectiveness of reusing steel slag powder and polypropylene fiber on the enhanced mechanical characteristics of cement-stabilized sand", *Civil Eng. Infrastruct. J.*, 1-19. https://doi.org/10.22059/CEIJ.2021.319310.1742.

Güllü, H. and Khudir, A. (2014), "Effect of freeze-thaw cycles on unconfined compressive strength of fine-grained soil treated with jute fiber, steel fiber and lime", *Cold Regions Sci. Tech*.,

106-107, 55-65. https://doi.org/10.1016/j.coldregions.2014.06.008.

Hadi Sahlabadi, S., Bayat, M., Mousivand, M. and Saadat, M. (2021), "Freeze–thaw durability of cement-stabilized soil reinforced with polypropylene/basalt fibers", *J. Mater. Civil Eng.*, **33**(9), 04021232. https://doi.org/10.1061/(asce)mt.1943-5533.0003905.

Heidarizadeh, Y., Lajevardi, S.H., Sharifipour, M. and Kamalian, M. (2021), "EExperimental characterization of the small strain shear modulus of soft clay stabilized with cement and nano-SiO2 using bender element tests", *Bull. Eng. Geol. Environ.*, **80**(3), 2523-2534. https://doi.org/10.1007/s10064-020-02096-z.

Irina, K. and Timo, K. (2014), "The effect of carbon fibers, glass fibers and nanoclay on wood flour-polypropylene composite properties", *Eur. J. Wood Wood Products*, **72**(1), 73-79. https://doi.org/10.1007/s00107-013-0754-8.

Jahandari, S., Li, J., Saberian, M. and Shahsavarigoughari, M. (2017), "Experimental study of the effects of geogrids on elasticity modulus, brittleness, strength, and stress-strain behavior of lime stabilized kaolinitic clay", *Geo. Res. J.*, **13**, 49-58. https://doi.org/10.1016/j.grj.2017.02.001.

Jassem, S. and Tabarsa, A. (2015), "Effect of adding nanoclay on the mechanical behaviour of fine-grained soil reinforced with polypropylene fibers", *J. Struct. Eng. Geotechnics*, **5**(2), 59-67.

Jiang, P., Chen, Y., Wang, W., Yang, J., Wang, H., Li, N. and Wang, W. (2022), "Flexural behavior evaluation and energy dissipation mechanisms of modified iron tailings powder incorporating cement and fibers subjected to freeze-thaw cycles", *J. Cleaner Product.*, **351**, 131527. https://doi.org/10.1016/j.jclepro.2022.131527.

Jiang, P., Zhou, L., Zhang, W., Wang, W. and Li, N. (2022), "Unconfined compressive strength and splitting tensile strength of lime soil modified by nano clay and polypropylene fiber", *Crystals*, **12**(2), 285. https://doi.org/10.3390/cryst12020285.

Kalhor, A., Ghazavi, M., Roustaei, M. and Mirhosseini, S.M. (2019), "Influence of nano-SiO 2 on geotechnical properties of fine soils subjected to freeze-thaw cycles", *Cold Reg. Sci. Tech.*, **161**, 129-136. https://doi.org/10.1016/j.coldregions.2019.03.011.

Kaniraj, S.R. and Havanagi,V.G. (2001), "Behavior of cement-stabilized fiber-reinforced fly ash-soil mixtures", *J. Geotech. Geoenviron. Eng.*, **127**(7), 574-584. https://doi.org/10.1016/10.1061/(asce)10900241(2001)127:7(574).

Kulanthaivel, P., Soundara, B., Velmurugan, S. and Naveenraj, V. (2021), "Experimental investigation on stabilization of clay soil using nano-materials and white cement", *Mater. Today: Proceedings*, **45**, 507-511. https://doi.org/10.1016/j.matpr.2020.02.107.

Li, H. and Senetakis, K. (2017), "Dynamic properties of polypropylene fibre-reinforced silica quarry sand", *Soil Dyn. Earthq. Eng.*, **100**, 224-232. https://doi.org/10.1016/j.soildyn.2017.05.035.

Liu, J., Bai, Y., Song, Z., Kanungo, D.P., Wang, Y., Bu, F., Chen, Z. and Shi, X. (2020), "Stabilization of sand using different types of short fibers and organic polymer", *Constr. Build. Mater.*, **253**, 119164. https://doi.org/10.1016/j.conbuildmat.2020.119164.

Liu, Y., Chang, C.W., Namdar, A., She, Y., Lin, C.H., Yuan, X. and Yang, Q. (2019), "Stabilization of expansive soil using cementing material from rice husk ash and calcium carbide residue", *Constr. Build. Mater.*, **221**, 1-11. https://doi.org/10.1016/j.conbuildmat.2019.05.157.

Lv, Q., Chang, C., Zhao, B. and Ma, B. (2018), "Loess soil stabilization by means of SiO2 nanoparticles", *Soil Mech. Found. Eng.*, **54**(6), 409-413. https://doi.org/10.1007/s11204-018-9488-2.

Momeni, M., Bayat, M. and Ajalloeian, R. (2022), "Laboratory investigation on the effects of pH-induced changes on geotechnical characteristics of clay soil", *Geomech. Geoeng.*, **17**(1), 188-196. https://doi.org/10.1080/17486025.2020.1716084.

Narani, S.S., Zare, P., Abbaspour, M., Fahimifar, A., Siddiqua, S. and Hosseini. S.M.M.M. (2021), "Evaluation of fiber-reinforced and cement-stabilized rammed-earth composite under cyclic loading", *Constr. Build. Mater.*, **296**, 123746. https://doi.org/10.1016/j.conbuildmat.2021.123746.

Olgun, M. (2013), "Effects of polypropylene fiber inclusion on the strength and volume change characteristics of cement-fly ash stabilized clay soil", *Geosynthetics Int.*, **20**(4), 263-275. https://doi.org/10.1680/gein.13.00016.

Orakoglu, M.E., Liu, J. and Niu, F. (2017), "Dynamic behavior of fiber-reinforced soil under freeze-thaw cycles", *Soil Dynam. Earthq. Eng.*, **101**, 269-284. https://doi.org/10.1016/j.soildyn.2017.07.022.

Phanikumar, B.R. and Ramanjaneya Raju, E. (2020), "Compaction and strength characteristics of an expansive clay stabilised with lime sludge and cement", *Soils Found.*, **60**(1), 129-138. doi: https://doi.org/10.1016/j.sandf.2020.01.007.

Pongsivasathit, S., Horpibulsuk, S. and Piyaphipat, S. (2019), "Assessment of mechanical properties of cement stabilized soils", *Case Studies Constr. Mater.*, **11**, e00301. https://doi.org/10.1016/j.cscm.2019.e00301.

Pu, S., Zhu, Z. and Huo, W. (2021), "Evaluation of engineering properties and environmental effect of recycled gypsum stabilized soil in geotechnical engineering: A comprehensive review", *Resour. Conserv. Recy.*, **174**, 105780.

Qi, J., Ma, W. and Song, C. (2008), "Influence of freeze-thaw on engineering properties of a silty soil", *Cold Reg. Sci. Tech.*, **53**(3), 397-404. https://doi.org/10.1016/j.coldregions.2007.05.010.

Michalowski, R.L. and Čermák, J. (2005), "Triaxial compression of sand reinforced with fibers", *J. Geotech. Geoenviron. Eng.*, **131**(January), 210-213.

Rezaei-Hosseinabadi, M.J., Bayat, M., Nadi, B. and Rahimi, A. (2022), "Utilisation of steel slag as a granular column to enhance the lateral load capacity of soil", *Geomech. Geoeng.*, **17**(5), 1406-1416. https://doi.org/10.1080/17486025.2021.1940315.

Roustaei, M., Hendry, M., Ali Aghaei, E. and Bayat, M. (2021), "Shear modulus and damping ratio of clay soil under repeated freeze-thaw cycles", *Acta Geodynamica et Geomaterialia* 18(1), 71-81. https://doi.org/10.13168/AGG.2021.0005.

Salehi, M., Bayat, M., Saadat, M. and Nasri, M. (2022), "PPrediction of unconfined compressive strength and California bearing capacity of cement-or lime-pozzolan-stabilised soil admixed with crushed stone waste", *Geomech. Geoeng.*, 18(4), 272-283. https://doi.org/10.1080/17486025.2022.2040606.

ShahriarKian, M.R., Kabiri, S. and Bayat, M. (2021), "Utilization of zeolite to improve the behavior of cement-stabilized soil", *Int. J. Geosynthetics Ground Eng.*, **7**(2), 35. https://doi.org/10.1007/s40891-021-00284-9.

Sharma, K. and Kumar, A. (2021), "Influence of rice husk ash, lime and cement on compaction and strength properties of copper slag", *Transport.Geotechnics*, **27**, 100464. https://doi.org/10.1016/j.trgeo.2020.100464.

Shibi, T. and Kamei, T. (2014), "Effect of freeze–thaw cycles on the strength and physical properties of cement-stabilised soil containing recycled bassanite and coal ash", *Cold Reg. Sci. Tech.*, **106-107**, 36-45. https://doi.org/10.1016/j.coldregions.2014.06.005.

Shokrieh, M.M., Saeedi, A. and Chitsazzadeh, M. (2013), "Mechanical properties of multi-walled carbon nanotube/polyester nanocomposites", *J. Nanostruct. Chem.*,

3(1). https://doi.org/10.1186/2193-8865-3-20.

Sukmak, P., Kunchariyakun, K., Sukmak, G., Horpibulsuk, S., Kassawat, S. and Arulrajah, A. (2019), "Strength and microstructure of palm oil fuel ash–fly ash–soft soil geopolymer masonry units", *J. Mater. Civil Eng.*, **31**(8), 04019164. https://doi.org/10.1061/(asce)mt.1943-5533.0002809.

Tang, C., Shi, B., Gao, W., Chen, F. and Cai, Y. (2007), "Strength and mechanical behavior of short polypropylene fiber reinforced and cement stabilized clayey soil", *Geotext. Geomembranes*, **25**(3), 194-202. https://doi.org/10.1016/j.geotexmem.2006.11.002.

Thomas, G. and Rangaswamy, K. (2020), "Dynamic soil properties of nanoparticles and bioenzyme treated soft clay", *Soil Dyn. Earthq. Eng.*, **137**. https://doi.org/10.1016/j.soildyn.2020.106324.

Tomar, A., Sharma, T. and Singh, S. (2019), "Strength properties and durability of clay soil treated with mixture of nano silica and polypropylene fiber", *Materials Today: Proceedings*, **26**, 3449-3457. https://doi.org/10.1016/j.matpr.2019.12.239.

Wang, T., Liu, Y., Yan, H. and Xu, L. (2015), "An experimental study on the mechanical properties of silty soils under repeated freeze-thaw cycles", *Cold Reg. Sci. Tech.*, **112**, 51-65. https://doi.org/10.1016/j.coldregions.2015.01.004.

Wang, X., Wu, Y., Lu, Y., Cui, J., Wang, X. and Zhu, C. (2021), "Strength and dilatancy of coral sand in the South China Sea", *Bull. Eng. Geol. Environ.,* **80**(10), 8279-8299. https://doi.org/10.1007/s10064-021-02348-6.

Yilmaz, Y. and Ozaydin, V. (2013), "Compaction and shear strength characteristics of colemanite ore waste modified active belite cement stabilized high plasticity soils", *Eng. Geol*., **155**, 45-53. https://doi.org/10.1016/j.enggeo.2013.01.003.

Yousefi, A., Aliaghaei, E., Kalhor, A., Jahanian, H. and Azadi, M. (2022), "The effect of freeze and thaw cycles on the dynamic properties of fine-grained soil Stabilized with nanocement", *Int. J. Geotech. Eng*., **16**(10), 1221-1233. https://doi.org/10.1080/19386362.2022.2106678.

Zhang, X., Gu, X., Lü, J. and Zhu, Z. (2016), "Experiment and simulation of creep performance of basalt fibre asphalt mortar under uniaxial compressive loadings", *J. Southeast Univ*., *(English Edition)*, **32**(4), 472-478. https://doi.org/10.3969/j.issn.1003-7985.2016.04.013.

CC